Mapping the urban microclimatic spatial distribution in a sub-tropical high-density urban environment

Yuan Shi[a*], Chao Ren[a,b,c], Yingsheng Zheng[a] and Edward Ng[a,b,c]

[a]*School of Architecture, The Chinese University of Hong Kong, Sha Tin, NT, People's Republic of China;* [b]*The Institute of Environment, Energy and Sustainability (IEES), The Chinese University of Hong Kong, Sha Tin, NT, People's Republic of China;* [c]*Institute Of Future Cities (IOFC), The Chinese University of Hong Kong, Sha Tin, NT, People's Republic of China*

(*Received 14 September 2014; accepted 3 October 2015*)

Understanding the urban microclimatic spatial distribution and its impact on thermal comfort is important for integrating climatic consideration into urban design process. This article presents a case study in Tsim Sha Tsui and Tai Po of Hong Kong densely built-up areas to investigate the spatial distribution of microclimatic condition. Air temperature (T_a), wind speed (v), relative humidity (RH) and globe temperature (T_g) of 87 locations in two selected sites were measured on a summer day and a winter day respectively. Physiological Equivalent Temperature was calculated to analyse the thermal comfort condition in two sites. Both numerical simulation and geographical mapping approach were used for the estimation of the microclimatic spatial distribution. Results show that the influence of urban morphology on the microclimatic spatial distribution can be well investigated by using numerical simulation while geographical mapping based on measured data shows higher estimation accuracy due to the consideration of anthropogenic heat and other factors associated with human activities. In summary, this article presents a pragmatic approach of mapping the urban microclimatic spatial distribution that can be referenced by architects and urban designers to raise climatic considerations for designing better cities.

Keywords: urban microclimate; spatial distribution; geographical mapping; ENVI-met; Physiological Equivalent Temperature (PET)

Introduction

Urban outdoor thermal environment serves an important function in urban living quality. People living in the cities, especially in mega-cities, are facing health threats resulting from urban heat island (UHI) effect and extreme weather conditions like heat waves caused by climate change and continuing urbanization (WHO 2003). According to the prediction of the United Nations Department of Economic and Social Affairs, the proportion of global urbanization will approximately be increased by 66.4% by 2050, with urban population reaching 6.3 billion by this time (UN 2014). Consequently, rising urban population implies an increasing vulnerability to the negative effects of climate change and urbanization.

Numerous studies have shown that urban planning and design-related factors such as land use and building morphology significantly affect urban microclimatic conditions (Crawford and Davoudi 2009). Sometimes, even a single building can affect the urban microclimate conditions of the entire neighbourhood. However, the integration of urban microclimatic considerations into design practices remains inadequate because it is not easy to find direct solutions from classical meteorological research due to interdisciplinary barriers. Moreover, training architects, urban planners and designers to design with regard to urban climate should be step-wise based on a systematic scheme (De Schiller and Evans 1996). Therefore, a quantitative and also intuitive understanding of spatial distribution of microclimate is essential for improving urban planning decision-making and design practices.

Mapping urban microclimate – the significance and objective

Urbanization physically transformed the natural land cover into a highly artificial environment which modifies local climatic conditions. Urban climatic studies are often conducted at three scales: mesoscale, local scale and microscale in descending order (Figure 1) (Oke 1997). A large number of previous urban climate studies concerning the spatial distribution of urban climate at mesoscale and local scale (Oke 1997, 2004). However, mapping the spatial distribution of meteorological parameters at microscale is even more important. Urban microclimate refers to the climatic conditions of a small-scale area in a city that may be distinctive with its surrounding areas and the

*Corresponding author. Email: shiyuan@link.cuhk.edu.hk

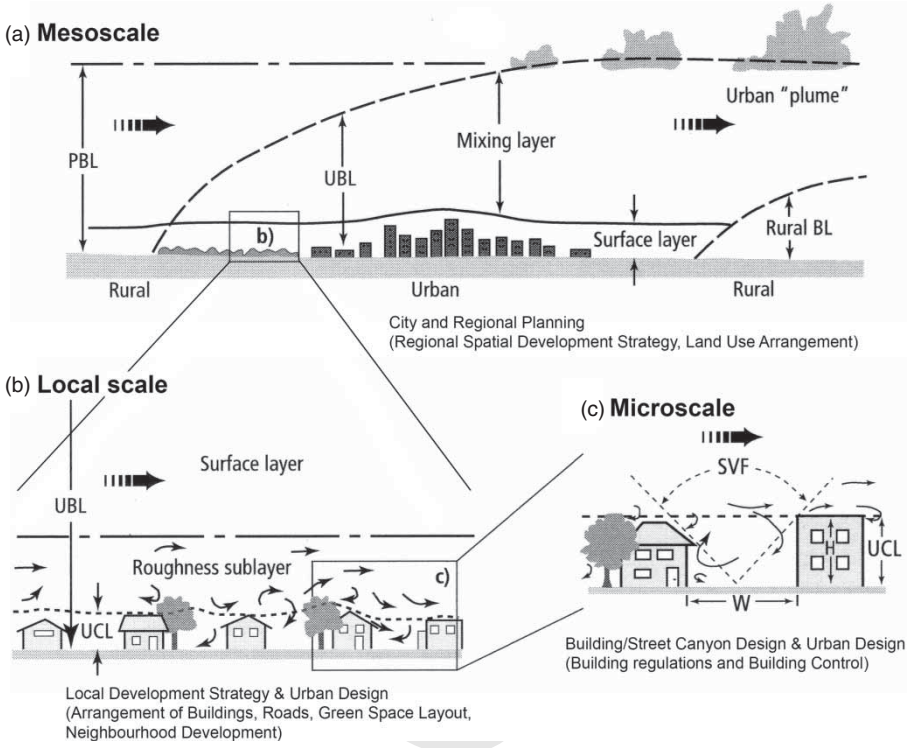

Figure 1. The different scales of urban climate and the corresponding links with architecture and urban planning scales. Source: modified from Oke (1997).

prevailing conditions of the whole city. Mapping urban microclimate reveals how the microclimate behaves within urban districts and between the buildings (Oke 1988; Erell, Pearlmutter, and Williamson 2011), which contributes to better understandings of its impacts on the outdoor thermal environment (Kántor and Unger 2010), human health (Oliveira and Andrade 2007) and building energy consumption (Santamouris et al. 2001) in a certain urban context. Mapping the spatial variation of microclimate can also provide useful information for public health research and management by identifying the hotspots of thermal discomfort so that individual thermal impacts can be evaluated. Therefore, increasing efforts have been made to explore the intra-urban variation of microclimatic conditions (Saaroni et al. 2000; Andrade and Alcoforado 2008; Chen et al. 2012). Recently the concept of Local Climatic Zone (LCZ) has been developed to quantify intra-urban microclimatic variations (Stewart and Oke 2012).

Spatially continuous data are essential to urban climatic studies as well as other environmental studies. However, acquiring these data through large-scale field measurements and long-term monitoring is time-consuming and expensive (Oke 2004; Li and Heap 2008). Several ways have been used to map the spatial distribution of meteorological parameters and obtain continuous data at different spatial scales, including scale model experiments like wind tunnel tests, remote sensing-based methods, numerical modelling like computer fluent dynamic simulation, and geographical mapping. Scale model experiments can generally provide accurate wind field information at the microclimate level. However, in most instances, thermal and radiant variables cannot be tested. Remote sensing data can be used to generate continuous spatial distribution of urban climate at mesoscale and local scale but it may not be adequate for microscale urban climatic studies since data of higher resolution are generally required. With the improvement of computational technology, the numerical modelling approach becomes more popular in studying urban microclimatic conditions (Robinson 2012). Geographical mapping is also one of the most commonly used methods for mapping the spatial distribution of environmental variables. This method has been used in several fields of environmental research such as biology, soil science, vegetation science and climatology (Hengl 2007; Huttner, Bruse, and Dostal 2008). In high-density urban environments, buildings do not only perturb airflows but also significantly alter the radiative balance which cannot be observed by most of the wind tunnel tests. High building density also hampers satellite imaging due to mutual masking between buildings. Therefore, in this study, numerical modelling and geographical mapping are used to develop a pragmatic approach of mapping the spatial variation of microclimate in the unique urban morphological conditions of Hong Kong in order to facilitate more climate-sensitive urban planning and design practices.

Study areas

Hong Kong (22° 150′ N, 114° 100′ E) is an international metropolis developed from an entrepôt city. It occupies an area of approximately 1100 km^2 and has a population of over seven million. It belongs to the sub-tropical maritime climate zone according to the Koppen Climate Classification and has hot humid summers and warm winters. According to the meteorological records of the Hong Kong Observatory (HKO), annual mean temperature and summer mean temperature are 23.3°C and 28.4°C respectively. Yearly mean of rainfall is 2398.5 mm.

Along with other mega-cities in the world, Hong Kong currently faces urban environmental issues and challenges such as UHI effect. Previous study revealed that an increase of 1°C in the daily mean temperature is associated with an estimated 1.8% increase in mortality (Chan et al. 2012). Meanwhile, Hong Kong is one of the most densely built cities that possesses irregular and complex urban morphology which significantly increases spatial variability in microclimate. Therefore, it is necessary not only to study urban climatic conditions at mesoscale and local scale, but also to explore the unique outdoor environment at microscale.

Two study areas, Tsim Sha Tsui and Tai Po, were selected for field measurements (Figure 2(a)). Tsim Sha Tsui is one of the central business districts located on the Kowloon peninsula. The western half of Tsim Sha Tsui area is occupied by densely built high-rise commercial and residential buildings while the eastern side contains several high-rise but less compacted buildings with a waterfront area in the southeast (Figure 2(b)). Vegetation is very limited in the open space along the main road through the centre of the study area and in the park at the southern part of the area. On the other hand, Tai Po is situated in the New Territories surrounded by hilly topography and neighbourhoods with relatively high density (Figure 2(c)). The eastern side of the study area has a large waterfront area and the whole study area contains different building types and several urban parks. According to the LCZ classification (Stewart and Oke 2012), the LCZ classes in the two selected areas, including compact high-rise, open high-rise, compact midrise, dense trees and low plants, can represent typical urban morphology of Hong Kong (Ren et al. 2015). The diversity in urban morphology of the two study areas is suitable for testing the proposed approaches of microclimatic mapping.

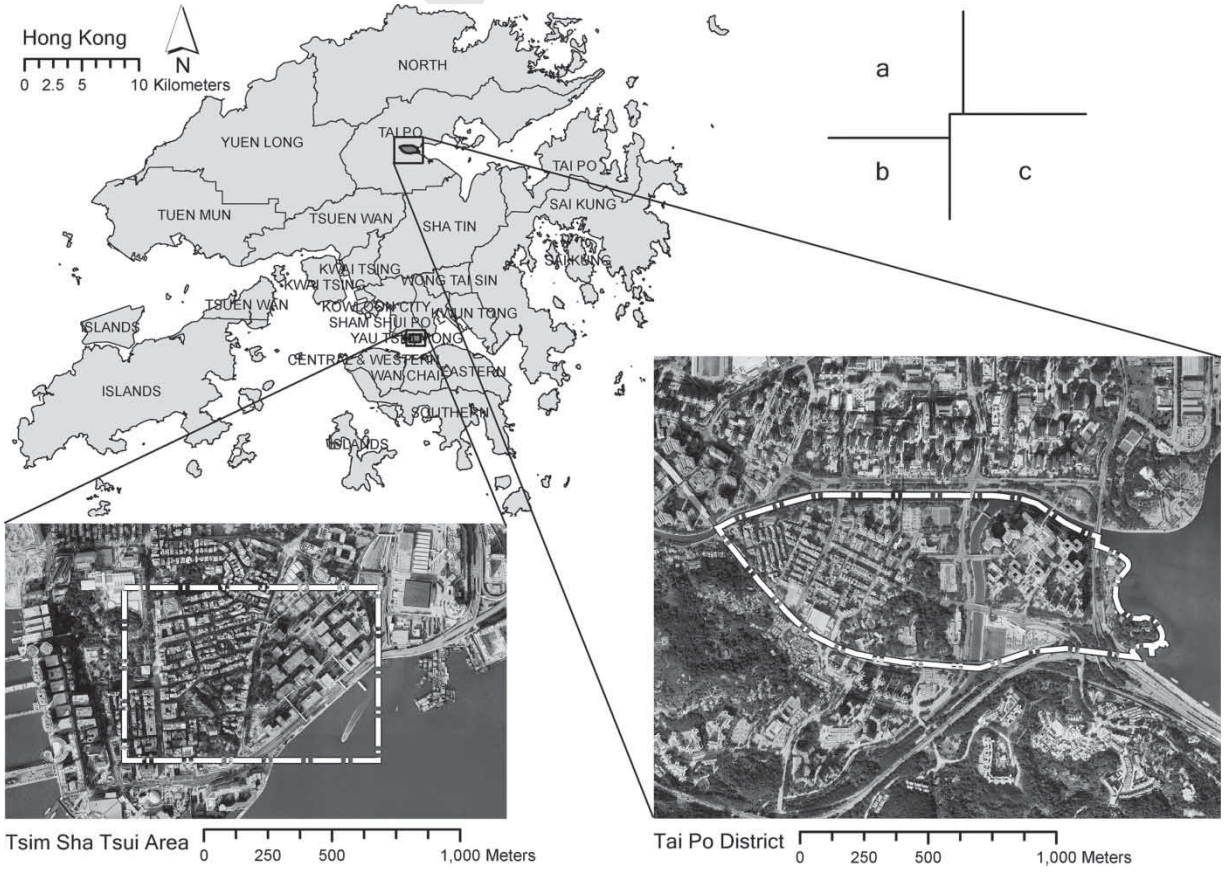

Figure 2. The location of two selected study areas in Hong Kong (a) and the aerial images of the Tsim Sha Tsui area (b) and Tai Po area (c), respectively.

Methodology

Field measurements were conducted to obtain information about air temperature (T_a), wind speed (v), relative humidity (RH) and globe temperature (T_g) in order to calculate the thermal comfort index – Physiological Equivalent Temperature (PET) at different locations in two selected areas (Höppe 1999). It is one of the most comprehensive thermal indices that has been used worldwide and in Hong Kong (Cheng et al. 2012; Ng and Cheng 2012). PET values calculated from measured data were then used for mapping the spatial variation of microclimate in a Geographical Information System (GIS) to generate spatially continuous distribution data.

Numerical simulation was also conducted to examine the effect of the irregular and complex urban and building morphology on the spatial distribution of microclimatic parameters by using a three-dimensional (3D) urban climatic model ENVI-met version 3.1 (Bruse 2009). The optimal microclimate mapping approach was determined through a comparison of the cross-validation results of different geographical mapping methods and the results of numerical simulation.

Field measurements and PET calculation

Field measurements

Field measurements were conducted to measure the T_a, v, RH and T_g of total 87 locations in the two study areas on a summer day and a winter day (Table 1). Background observed data during all measurement periods were also collected from meteorological stations operated by the HKO for reference.

Measurement equipment and data sampling

Microclimatic conditions of each test point were measured with a mobile meteorological station (Figure 3). T_a, v, and RH are directly measured by the TESTO 400 three-function sensor probe. Mean radiant temperature (T_{mrt}), as a microclimatic element for predicting thermal comfort, was calculated from T_g (ISO 1998), which is measured by a TESTO flexible Teflon type K thermocouple wire fixed at the centre of a 38-mm black globe (Humphreys 1977; Nikolopoulou, Baker, and Steemers 1999).

The mobile meteorological station was set up at each test point at a height of 2 m for 5 min. 5-min mean values of T_a, v, RH, and T_g were then calculated from the measured data. After the 5-min sampling, the station was moved to the next test point and the time interval between two test points was 10–15 min.

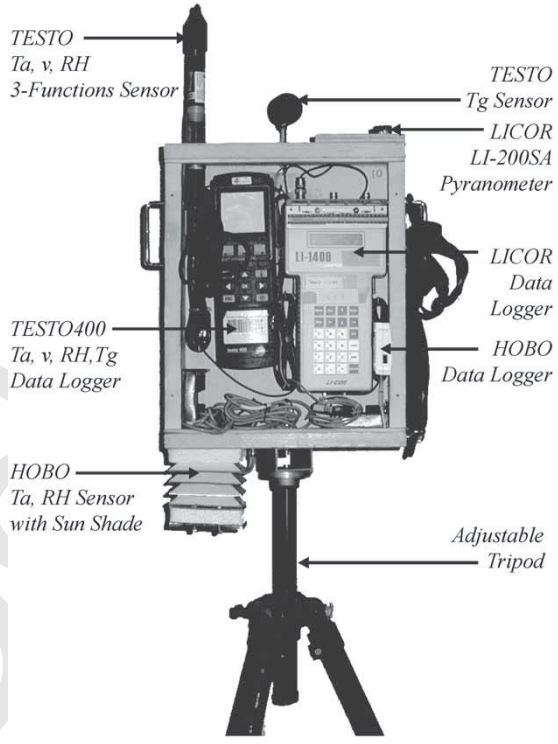

Figure 3. The mobile meteorological station used in this study.

Measurement network

The distribution of test points is arranged according to the following conditions: (1) all test points should be in full outdoor space, avoiding semi-outdoor spaces like inner courtyards; (2) all test points should be evenly distributed and (3) fixed reference points should be set up on the windward side of prevailing wind direction during the measurement period such that background climatic conditions of the study area can be simultaneously recorded throughout the entire measurement period. All test points for each study area were pre-selected and measured by individual groups so that all measurements could be completed within 1–2 hours. Figure 4 shows the measurement network of the two study areas.

Data usability

Mapping of the spatial distribution requires relatively stable background weather conditions during the whole

Table 1. Basic information of the field measurement of on two study areas.

Site	Measurement date	Measurement time	Weather condition	Total test points no.
Tsim Sha Tsui	9 September 2008	14:30–15:30 (1 h)	Typical summer day, No rainfall	13
Tai Po	13 January 2014	12:00–14:00 (2 h)	Typical winter day, no rainfall	74

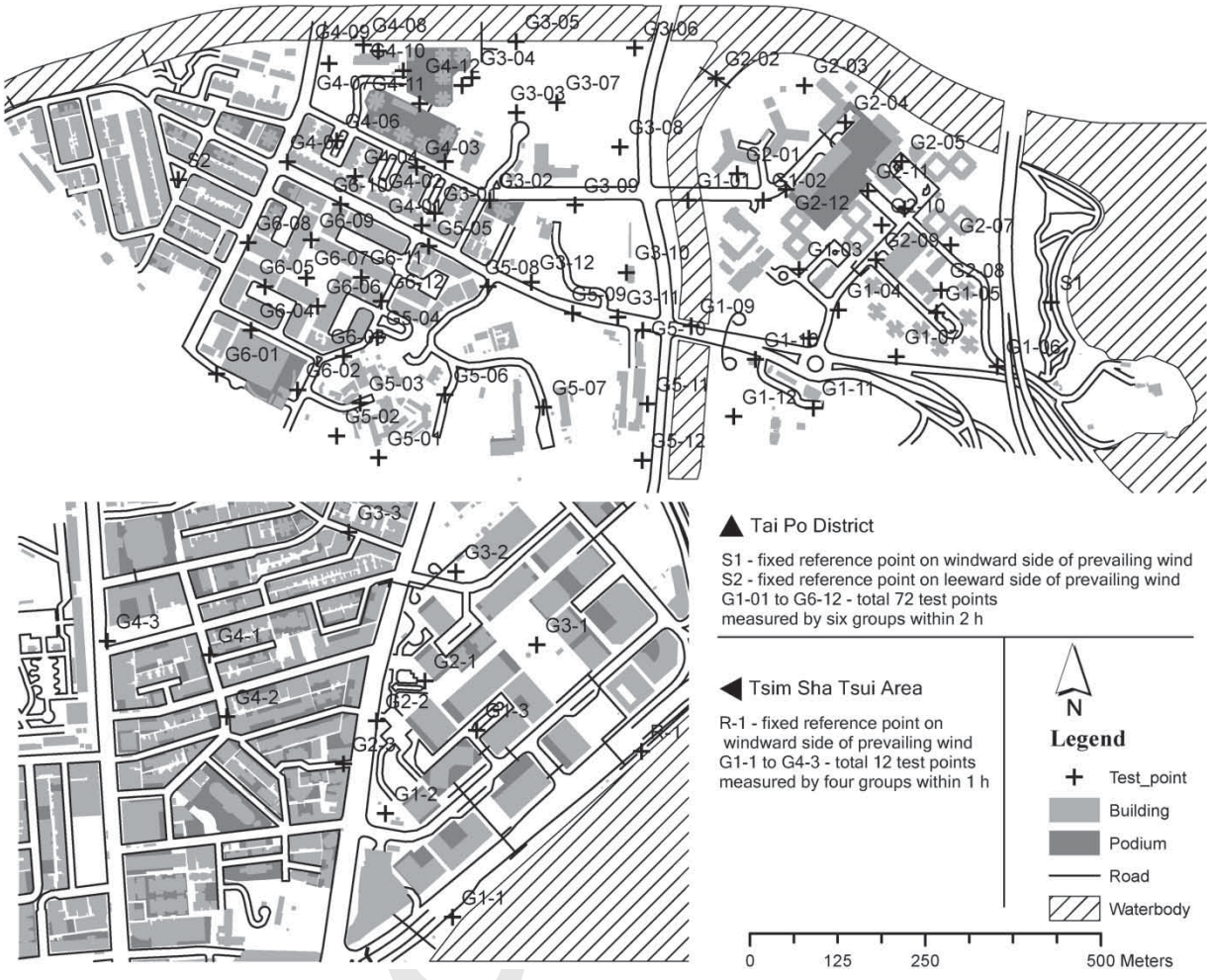

Figure 4. The measurement network (the spatial distribution of test points) of the Tsim Sha Tsui area and Tai Po area.

measurement period (i.e. the temporal variation of the background weather condition should be insignificant when compared with the spatial variation of data from all test points).

The standard deviations (SD) of T_a, v, RH, and T_g from different data sources were calculated. Comparison between HKO records, temporal data measured at fixed reference points and data measured at other test points during the measurement period show that the temporal variation of background weather data during the measurement period was relatively insignificant compared with the spatial variation of measured data for both of two areas (Tables 2 and 3). Therefore, data from different test points are dependable for spatial distribution mapping.

Table 2. Comparison of SD of background weather data and measurement data in Tsim Sha Tsui area.

	v (m/s)	T_a (°C)	RH (%)
HKO station (temporal variation at HKO and King's park stations)	0.21	0.22	0.65
Reference point R-1 (temporal variation)	0.08	0.21	0.72
12 test points (spatial variation)	0.78	1.33	3.82

PET calculation

PET – a universal index for the biometeorological assessment of the thermal environment is selected as the principal thermal comfort index in this study (Mayer and Höppe 1987; Höppe 1999). The Munich Energy-Balance Model for Individuals (MEMI) was developed on the basis of bioclimatological knowledge of the human body's energy balance. According to the MEMI, PET can be calculated from T_a (°C), v, (m/s), T_{mrt} (°C), water vapour pressure (p_a, hPa), metabolic rate and clothing index. T_a and v are directly measured. T_{mrt} is calculated by using the measured T_g based on the following equation (ISO 1998;

Table 3. Comparison of SD of background weather data and measurement data in Tai Po area.

	v (m/s)	T_a (°C)	RH (%)
HKO station (temporal variation at Tai Po Station)	0.41	0.29	1.35
Reference point S1 (temporal variation)	0.06	0.22	0.82
Reference point S2 (temporal variation)	0.25	0.50	1.04
72 test points (spatial variation)	1.77	4.29	14.67

ASHRAE 2004):

$$T_{\mathrm{mrt}} = \left[(T_g + 273.15)^4 + \frac{1.10^{*}10^{8*}v^{0.6}}{\varepsilon^{*}D^{0.4}}(T_g - T_a)\right]^{1/4} - 273.15,$$

where ε is the emissivity of the globe (0.95 for a black globe); D is the globe diameter (38 mm in this study); T_a is air temperature (°C); T_g is globe temperature measured by globe thermometer (°C); v is wind speed (m/s). p_a was calculated from measured T_a and RH by using following equation (Cena and Clark 1981):

$$p_a = \mathrm{RH}^{*}10^{*}\exp\left(16.6536 - \frac{4030.183}{T_a + 235}\right).$$

The most typical pedestrian walking speed for a commercial and residential mixed-use district is 3 km/h (Penwarden and Wise 1975), which can be regarded as slow walking with a metabolic rate of 2.0 met. Clothing index was set to 0.3 and 1.2 clo for summer and winter respectively. Based on the above equations and assumptions, PET values for all 87 test points at the two study areas were calculated.

ENVI-met simulation

ENVI-met, a three-dimensional numerical urban microclimate model developed for simulating surface–plant–air interactions inside urban environments, was used in this study (Bruse and Fleer 1998). The main advantage of ENVI-met is that it provides an integral solution of numerical simulation particularly programmed to simulate an urban microclimate using fluid dynamics, thermodynamics and urban meteorology (Bruse 1999). Therefore, the interaction between urban morphologies and urban microclimate can be independently simulated under controlled circumstances without the effect of other factors.

Model input and simulation settings

Simulation domains of the two study areas were created in ENVI-met Eddi model editor. In the simulation domain, buildings, plants and soil layers are edited in the modelled area grids according to information obtained from the GIS database acquired from the Hong Kong Planning Department. Building shape was moderately simplified after importation to avoid captured grids which cause instability problems during iterations of the simulation (Bruse 2009). Different domain sizes and spatial resolution were tested for balancing the coverage of modelled area and the accuracy of the spatial model in order to finalize the modelled area of the two study areas (Figure 5). Nesting grids were added around the modelled area to provide appropriate buffer space between buildings and the boundary of the simulation domain. Vertical grids were generated using telescoping algorithm so that more layers can be generated within the pedestrian level for more accurate results. Receptors were added to the corresponding locations of all test points in the modelled area to extract the value of simulated microclimatic variables at the pedestrian level height (2 m above ground) which is consistent with previous studies in Hong Kong (Ng 2009).

Initial wind conditions, thermal conditions and soil temperature were set for two sites respectively according to the background weather data during the field measurement period obtained from neighbouring HKO meteorological stations (Tables 4 and 5). Wind speed data provided by relevant HKO stations are obtained at different height depending on the height of anemometers above the ground. The configuration of ENVI-met requires the wind speed at 10 m above the ground level as the input. Therefore, the wind speed from HKO was adjusted using power law wind profile (Santamouris and Allard 1998):

$$\frac{U_{10}}{U_{\mathrm{HKO}}} = \mathrm{K}z^{\alpha},$$

where U_{10} is the wind speed at 10 m height which will be used as the input for ENVI-met; U_{HKO} is the wind speed measure at anemometer height of corresponding HKO meteorological station; z is the required height which is 10 m for ENVI-met input; Both coefficient K and exponent α are terrain dependent constants with the value of 0.21 and 0.33 for the urban environment.

Both the building properties and bioclimatic parameters were configured for the model. Simulation settings (Table 6) based on the Hong Kong built environment used in previous research were adopted (Ng et al. 2012).

Simulation results

Building geometry has a significant influence on urban microclimate because buildings in urban areas block the open sky and consequently change the radiation balance in the urban environment. Sky view factor (SVF, ψ_s) is an indicator to describe the building geometry that has been widely used to indicate the impact of urban morphology on the microclimatic conditions (Oke 1981; Svensson 2004).

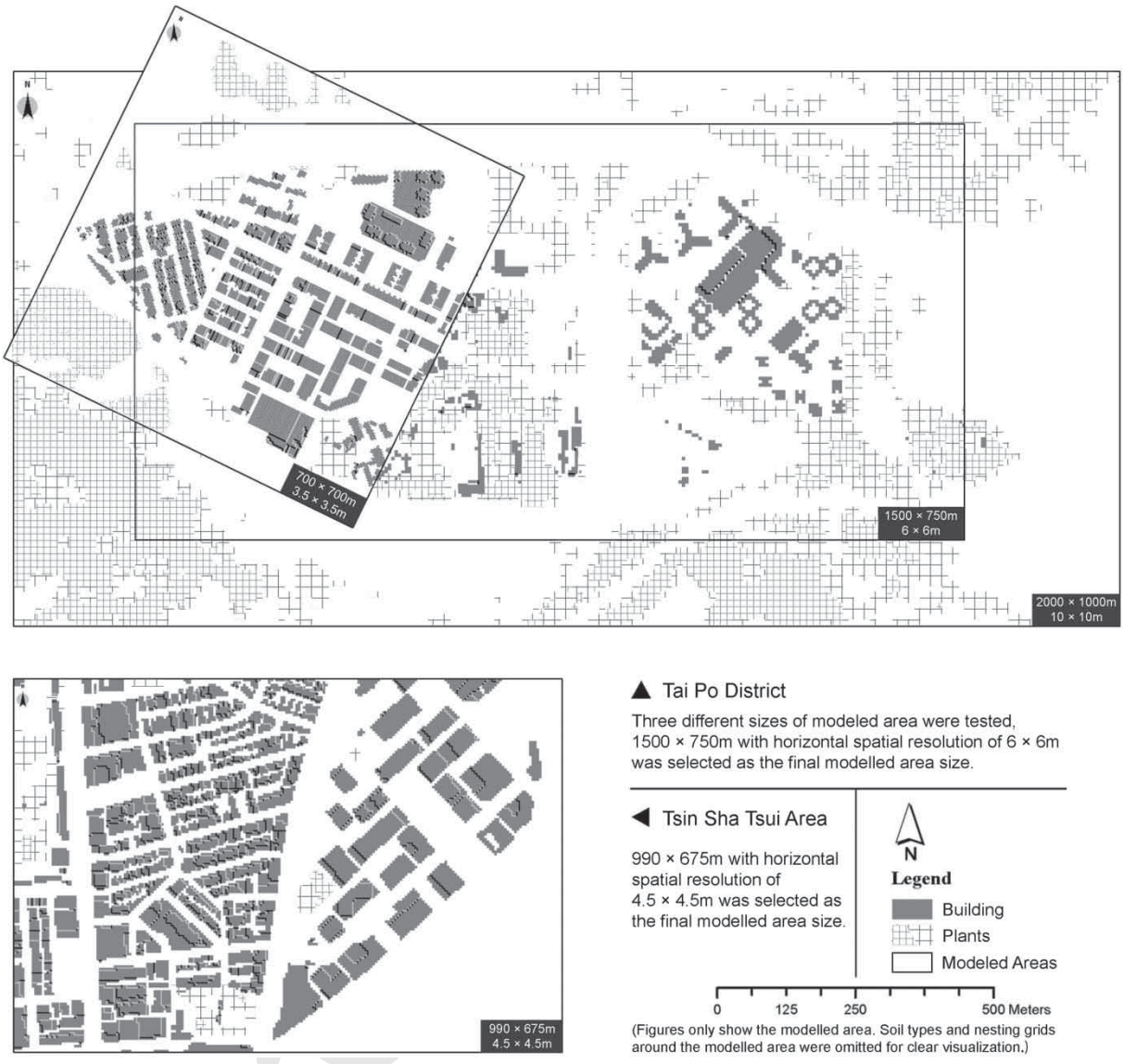

Figure 5. Snapshot of modelled area of two study areas in ENVI-met model domain.

Table 4. Basic background weather data at Tsim Sha Tsui area during measurement period and corresponding settings in ENVI-met configuration.

During 14:30–15:30 9 September 2008	HKO meteorological records	ENVI-met settings
Wind speed (m/s)	3.47–3.83	2.41 (adjusted to 10 m level)
Wind direction	ESE	112.5° (N = 0°, E = 90°)
Temp (°C)	32–32.5	Daily minimum
RH (%)	61–62.6	61 (mean)

Table 5. Basic background weather data at Tai Po area during measurement period and corresponding settings in ENVI-met configuration.

During 12:00–14:00 13 January 2014	HKO meteorological records	ENVI-met settings
Wind speed (m/s)	4.86–5.73	2.72 (adjusted to 10 m level)
Wind direction	WNW–NW	300° (N = 0°, E = 90°)
Temp (°C)	13.7–14.5	Daily minimum
RH (%)	52–56	53.8 (mean)

SVF also defines the ratio between radiation received by a planar surface (in urban street canyons, building clusters) and that from the entire hemispheric radiating environment (the open sky) (Watson and Johnson 1987). Based on the 3D GIS data set of the two study areas, the SVF values of all test points were calculated by using an existing VBA

Table 6. Configurations of building properties and bioclimatological parameters in ENVI-met model.

Parameters	Tai Po station of HKO	ENVI-met settings
Building properties	Albedo of roofs	0.3
	Albedo of walls	0.2
Required input for thermal index	Walking speed (m/s)	0.8
	Energy-exchange (Col. 2 M/A)	116
	Mech. factor	0.0
	Heat transfer resistance cloths	0.3(summer), 1.2(winter)

computer program developed and embedded as a macro in the ArcGIS system (Chen et al. 2012) and also by using the ENVI-met. The comparison between the SVF values calculated from the two methods shows that the rasterized ENVI-met input models can represent the real urban geometry of the two study areas very well with the high R^2 of 0.976 and 0.915 for Tsim Sha Tsui and Tai Po respectively (Figure 6).

This study aims to assess the performance of the ENVI-met model by comparing modelled data to data obtained during the measurement period. According to Bruse (2009), the simulation of the two study areas were run for 24 h starting from 6 am and modelled data during the initialization of the model were discarded. Data recorded by pre-distributed receptors in the ENVI-met model domain during corresponding measurement period were extracted for further analysis. A previous study using ENVI-met simulation in a relatively small area with simple building geometry and vegetation shows reasonable agreement between measured and modelled T_{mrt} data with R^2 of 0.615–0.745 (Chen and Ng 2012). In the present study with two larger modelled areas and more complex urban morphology, the comparison between measured and modelled PET data does not show very good agreement with R^2 of 0.293 and 0.227 for Tsim Sha Tsui and Tai Po respectively (Figure 7). The ENVI-met model is specially developed to focus on the modelling of plant–surface–air interactions and suitable for parametric simulation of the relationship between urban microclimate and urban morphology or cases that are dominated by the effect of building geometry and plants (Ng et al. 2012). Anthropogenic heat released from intensive use of building equipment and dense traffic flows are not fully taken into account at the present stage. However, both of the areas in this study are not only affected by building geometry and vegetation, but also affected by in-situ anthropogenic heat release. It has been proved that anthropogenic heat has large impacts on the urban climate and thermal environment because it plays an important role in the urban energy balance (Ichinose, Shimodozono, and Hanaki 1999; Fan and Sailor 2005; Kato and Yamaguchi 2005). According to Man Sing et al. (2015), the influence of anthropogenic heat is more significant in the two study areas due to the high building density in the urban area of Hong Kong. Therefore, the relatively weak correlation between measured and modelled data is possibly due to the anthropogenic heat release in the two study areas. Although the agreement between measured and simulated data may be affected by anthropogenic heat, the comparison result implies that the building geometries do have an influence on the microclimatic variation that cannot be ignored. Because that the agreements with R^2

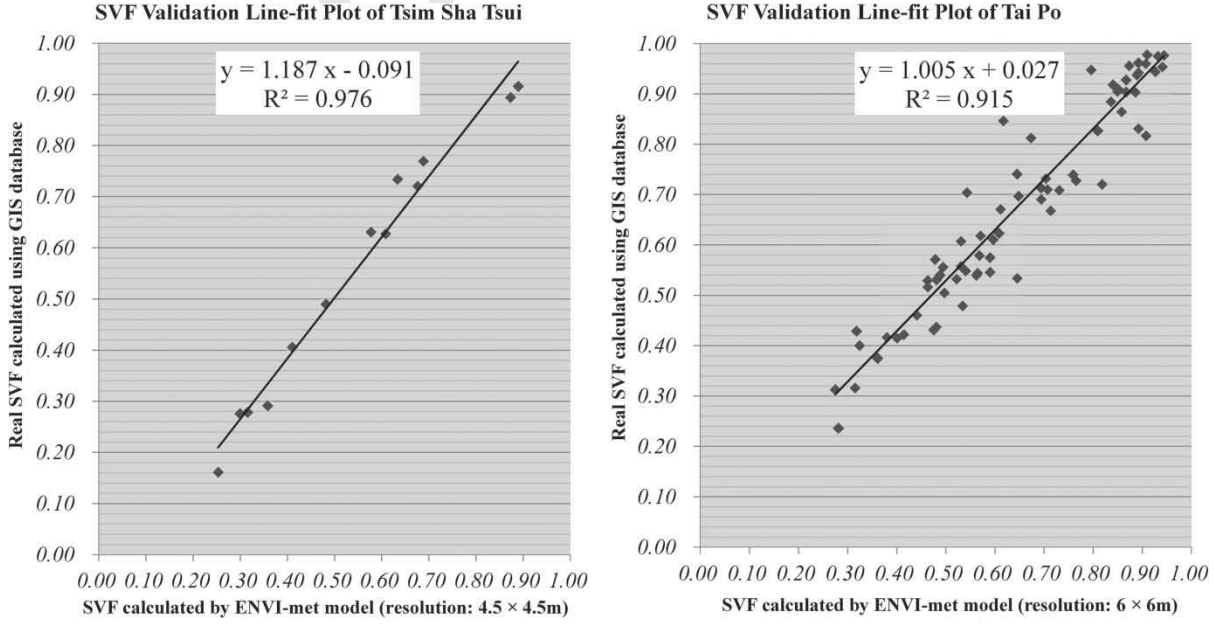

Figure 6. Comparison of the ENVI-met-calculated SVF and GIS-calculated SVF.

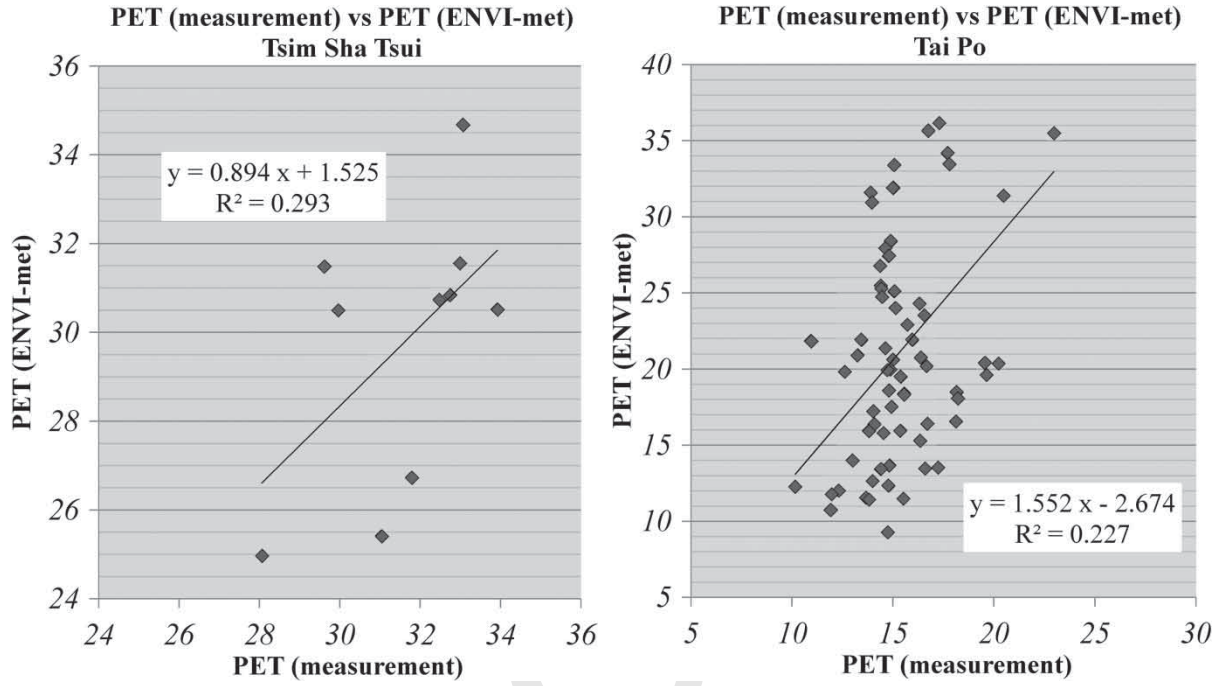

Figure 7. Comparison of the PET simulated by ENVI-met model and PET calculated using measurement data.

of 0.293 and 0.227 between measurement and simulation imply that the simulated data statistically interpret 20–30% of the characteristic of measured data.

Geographical mapping

Mapping the urban microclimatic distribution for urban areas by using measured data can also take anthropogenic heat into account for better estimation. Spatial interpolation is the principal method of geographical mapping used in this study. There are generally two types of spatial interpolation including deterministic interpolation and stochastic interpolation method according to basic interpolation theory (Boer, de Beurs, and Hartkamp 2001). Deterministic interpolation is known as non-geostatistical interpolation while stochastic interpolation refers to geostatistical interpolation in other studies (Andy, 2005). Spatial interpolation techniques are used to generate spatially continuous data of climatic variables (Hartkamp et al. 1999) at both regional scale (Apaydin, Sonmez, and Yildirim 2004) and intra-urban scale (Zhang et al. 2011). These previous studies do not only acquire spatially continuous data but also suggest optimal interpolation methods for further studies on other similar cases. However, Hong Kong has a distinctive urban morphology so interpolation methods recommended by previous studies may be unsuitable for such a unique urban environment. Therefore, different spatial interpolation methods must be compared before mapping the spatial distribution of microclimatic variables in Hong Kong.

Seven types (22 subtypes) of spatial interpolation techniques were tested to explore the spatial distribution of two basic climatic parameters, namely T_a and RH, as well as the thermal index PET. The reason for choosing T_a and RH is that both of the parameters are the most basic meteorological parameters for meteorological observations and daily weather forecast. As mentioned, PET was chosen as the proxy of the spatial distribution of microclimatic variables due to the following reasons: (1) PET calculation is based on the MEMI human physiological model which is the most comprehensive model to evaluate the heat balance of the human body; (2) PET has been commonly used for microclimate studies worldwide and particularly in tropical climate like Hong Kong (Chen and Ng 2012; Cheng et al. 2012). The effects of building geometry, waterbodies and plants were also considered during interpolation. Implementation of different types of interpolation approaches is based on previous studies and several practical guides (Webster and Oliver 2001; Hengl 2007).

Local polynomial interpolation

Local polynomial interpolation (LPI) is defined in relation to global polynomial interpolation (GPI). LPI uses multiple polynomials to fit the entire data surface, whereas GPI uses only one single polynomial to fit the data surface (Johnston et al. 2001). LPI allows the interpolation model to represent several details on local variations within the study area which may be useful for exploring the highly variable urban context of Hong Kong.

Kriging and CoKriging

Kriging has numerous interpolation subtypes such as original kriging (KO), universal kriging (KU), simple kriging (KS), and disjunctive kriging (KD). KO is widely adopted to create spatially continuous data of climatic variables (Hartkamp et al. 1999). A semivariogram model is used in KO to estimate the value of climatic variables at an unmeasured point based on the values of neighbouring measured points (Nalder and Wein 1998). KU uses the same theory. Additionally, KU removes the overall data trend of the study area before interpolation and adds them back before creating the spatially continuous data (Cressie 1986; Johnston et al. 2001). The difference between KS and KO is similar to the difference between GPI and LPI. KD has the lowest tolerance for measurement errors and assumes bivariate normality. Therefore, the KS and KD were not used in this study. Cokriging considers additional variables that exhibit inter-correlations which possibly produces better performance than kriging with highly correlated covariates (Johnston et al. 2001). Similarly, cokriging also has two subtypes including original cokriging (CKO) and universal cokriging (CKU).

Interpolation with barriers

Interpolation with barriers is an interpolation method that can directly estimate the effect of physical barriers within the study area into the interpolation procedure. Two types of barriers-incorporated interpolation methods were used in this study, which are kernel interpolation and diffusion interpolation with barriers. Kernel interpolation can adjust the estimates for barriers based on symmetric kernels such as exponential or Gaussian so more accurate prediction around barriers can be obtained. Diffusion interpolation estimates spatial distribution around the barriers by using the fundamental solutions of heat and particle diffusion equations. The specific algorithms of barriers-incorporated interpolation methods are complex and have been described in a previous study (Johnston et al. 2001). Considering the effect of physical barriers could possibly improve the performance of interpolation in the present study because of the influence of building geometry in such a dense built environment.

Cross validation

Cross validation was used to evaluate the performance of different interpolation methods and compare prediction results. In this method, one of the test points used in field measurement is provisionally removed. The parameter's value of interest at this point is predicted by using the model generated during the interpolation process. The differential between the measured and predicted values is the predicted error. This procedure is repeated for each test point. The root mean square error (RMSE) of these predicted values was calculated as the index for the comparison of model performance according to the following equation:

$$\mathrm{RMSE} = \sqrt{\frac{1}{n}\sum_{i=1}^{n}(y_i - \hat{y}_i)^2},$$

where y_i is the measured value of the specific parameter at test point i, $\hat{y}_i$ is the predicted value at the same point acquired by using the interpolation model, and n is total number of test points. The RMSE of the simulation results of the ENVI-met model were also calculated to compare the prediction accuracy of microclimate modelling and geographical mapping.

Spatial interpolation and result analysis

The polynomial used in the spatial interpolation process is based on a kernel function. Six types of kernel functions were tested using the three variables (T_a, RH and PET) of both Tsim Sha Tsui and Tai Po to determine the optimal kernel function for each variable for the purpose of getting the minimum interpolation error (as mentioned, represented by RMSE in this study). The result (Table 7) shows the RMSE of using six types of kernel functions for T_a, RH and PET of the two study areas. Kernel functions

Table 7. RMSE comparison of predicted parameters by LPI methods based on different kernel function. The minimum RMSE values of different variables of different sites were italicized.

	Study area					
	Tsim Sha Tsui			Tai Po		
Kernal functions	RMSE (T_a, °C)	RMSE (RH, %)	RMSE (PET, °C)	RMSE (T_a, °C)	RMSE (RH, %)	RMSE (PET, °C)
Exponential	0.964	5.33	2.131	*0.878*	4.28	2.643
Gaussian	0.945	5.37	2.152	0.884	3.85	2.679
Polynomial5	0.934	5.53	2.261	0.889	3.94	2.653
Epanechnikov	0.920	5.39	2.170	0.886	*3.58*	2.594
Quartic	0.932	5.43	2.206	0.888	3.91	2.641
Constant	*0.916*	*5.30*	*2.009*	0.923	4.31	*2.592*

that produce the minimum RMSE were used for further mapping process.

Seven types of spatial interpolation methods were tested for spatial interpolation and unmeasured area predictions after determining the kernel function for each variable of interest. The effects of urban geometry, waterbody and greening were also examined. These parameters were used as weight factors for LPI or as covariates of cokriging. Therefore, 22 subtypes of interpolation method were used for the interpolation of three parameters of interest (Table 8). The RMSE of the prediction errors of all 22 method subtypes were classified in two different ways: different interpolation methods and consideration of weight factors/covariates. The average RMSE was used to compare the performance of different methods.

Table 8. List of 22 types of tested spatial interpolation methods. The method column: Local polynomial interpolation (LPI), Original kriging (KO), Universal kriging (KU), Original Cokriging (CKO), Universal Cokriging (CKU), Kernel interpolation with barriers (KIB) and Diffusion interpolation with barriers (DIB); The weight factors and covariates: 1-sky view factor (SVF), 2-distance to waterbody and 3-distance to plants.

Code	Alias	Method	Weight factors	Covariates
a	LPI	LPI	none	N/A
b	LPIS	LPI	1	N/A
c	LPIW	LPI	2	N/A
d	LPIP	LPI	3	N/A
e	KO	KO	N/A	none
f	CKOS	CKO	N/A	1
g	CKOW	CKO	N/A	2
h	CKOP	CKO	N/A	3
i	CKOA	CKO	N/A	1,2,3
j	KU	KU	N/A	none
k	CKUS	CKU	N/A	1
l	CKUW	CKU	N/A	2
m	CKUP	CKU	N/A	3
n	CKUA	CKU	N/A	1,2,3
o	KIB	KIB	none	N/A
p	KIBS	KIB	1	N/A
q	KIBW	KIB	2	N/A
r	KIBP	KIB	3	N/A
s	DIB	DIB	none	N/A
t	KIBS	DIB	1	N/A
u	KIBW	DIB	2	N/A
v	KIBP	DIB	3	N/A

Comparing different interpolation methods

Table 9 shows the results and a comparison of the average RMSE of predicted values among the seven interpolation methods. The CKO method produces the minimum RMSE for almost all parameters of interest, which means that, overall, the CKO method shows the best estimation accuracy among all methods in this study.

Identifying dominant microclimate impact factors

Table 10 shows the results and a comparison of the average RMSE of predicted values produced by considering the different weight factors or covariates. Interpolation models show better performance when the effects of urban geometry, waterbody, or urban greening were considered in the interpolation model either by using them as weight factors for LPI or as covariates for cokriging for both study areas. However, their dominant weight factors or covariates are slightly different. As regards T_a, the dominant covariate for cokriging interpolation of Tsim Sha Tsui and Tai Po are SVF and the distance to greening area respectively. For Tsim Sha Tsui, the high correlations between T_a, PET and SVF indicates that the thermal index is dominated by building geometry in high-density building environment, especially in the scenario of lacking urban greening. Regarding the Tai Po area, it is reasonable that the dominant factor for T_a is the distance to greening area due to the much higher greenery coverage ratio and lower building density. As to the RH, results show that comprehensively integrating all three factors (SVF, distance to waterbody, and plants) into the interpolation provided the most accurate predictions. As regard to PET, the PET variation in the densely-built Tsim Sha Tsui is dominated by building geometry. In contrast, the spatial

Table 9. Comparison of the RMSE of predicted parameters by different interpolation methods. The minimum RMSE mean values were italicized.

	Study area					
	Tsim Sha Tsui			Tai Po		
Methods	RMSE (T_a, °C)	RMSE (RH, %)	RMSE (PET, °C)	RMSE (T_a, °C)	RMSE (RH, %)	RMSE (PET, °C)
LPI	0.952	5.52	2.214	0.821	3.32	2.634
KO	0.789	5.37	2.152	0.761	3.06	2.547
CKO	*0.702*	*2.42*	2.037	*0.759*	*3.05*	*2.513*
KU	0.789	2.42	*1.952*	0.777	3.36	2.533
CKU	1.076	3.23	2.315	0.830	3.37	2.549
KIB	0.774	3.23	2.173	0.820	3.45	2.563
DIB	1.040	3.82	2.189	0.930	3.56	2.535

Table 10. Comparison of the RMSE of predicted parameters by the consideration either on different weight factors or different covariates. The minimum RMSE mean values were italicized.

	Study Area					
	Tsim Sha Tsui			Tai Po		
Covariates/weight factors	RMSE mean (T_a, °C)	RMSE mean (RH, %)	RMSE mean (PET, °C)	RMSE mean (T_a, °C)	RMSE mean (RH, %)	RMSE mean (PET, °C)
None	0.951	4.65	2.150	0.851	3.43	2.574
SVF (1)	*0.898*	5.21	*2.104*	0.826	3.34	2.573
Waterbody (2)	1.090	4.34	2.389	0.816	3.29	2.531
plants (3)	0.899	5.29	2.490	*0.814*	3.35	2.497
all (1,2,3)	1.155	*3.67*	3.205	0.825	*3.21*	*2.491*

variation of PET in Tai Po is comprehensively affected by building geometry, waterbody and urban vegetation. In summary, the consideration of building geometry, waterbody, and greening indeed reduced the prediction RMSE of all parameters of interest. However, the most essential weight factor or covariate for microclimate interpolation of different areas may be diverse because of the dominant impact factors of microclimatic spatial variation depend on the characteristics of different sites.

Conclusion and discussion

By focusing on how to make use of real measured data to generate more reliable spatially continuous data for the purpose of getting better estimation of microclimate spatial distribution in sub-tropical high-density urban environment, geographical mapping method was applied for an improved estimation of microclimatic spatial distribution in this study. A comparison of prediction errors produced by 22 subtypes of geo-spatial interpolation methods revealed that CKO, integrated with urban geometry, waterbody and greening, is an optimized method for microclimatic spatial distribution estimation in high-density urban areas with complex morphology. Compared with the numerical simulation, the prediction error of microclimatic variables was significantly reduced when the geographical interpolation method based on real measured data was used to take the anthropogenic heat and other human activities relevant impact factors in real complex urban context into account (Table 11). Such reduction is essential to the urban microclimatic environmental assessment.

The connection between urban microclimate mapping and architectural practice

The mapping of urban microclimate is vital to the urban environmental studies and architectural and planning practices, especially for the high-density built environment because buildings can significantly change the climatic conditions prevailing over urban areas by disturbing the airflows passing through the urban fragments and modifying the radiation balance schemes within the street canyon. The interactions between architectural practices and urban microclimate are much stronger than the practitioners expected. The effects of urban microclimate are associated with a wide range of environmental issues like climate change and extreme weather becomes much more threatening to people living in cities. Therefore, there is an urgent need of taking urban microclimate into architectural and planning considerations.

In Hong Kong, with increasing awareness of using climatic knowledge in urban planning and architectural design, efforts have been made to build the interdisciplinary bridge between science and design (Ng 2012). Urban Climatic Map (Ng, Cheng, and Chan 2008; Ng and Ren 2012) and Air Ventilation Assessment (AVA) (Ng 2009) provide the climatic information platform and the implementation control guideline for better planning and design implemented at mesoscale and local scale

Table 11. Comparison of the RMSE of predicted parameters by different interpolation methods. The minimum RMSE values produced by geographical interpolation method for each microclimate variables were selected for the comparison.

	Study area					
	Tsim Sha Tsui			Tai Po		
Methods	RMSE mean (T_a, °C)	RMSE mean (RH, %)	RMSE mean (PET, °C)	RMSE mean (T_a, °C)	RMSE mean (RH, %)	RMSE mean (PET, °C)
Geographical mapping	0.702	2.42	1.816	0.746	2.98	2.490
Numerical simulation	1.243	3.71	3.057	1.370	5.72	7.424

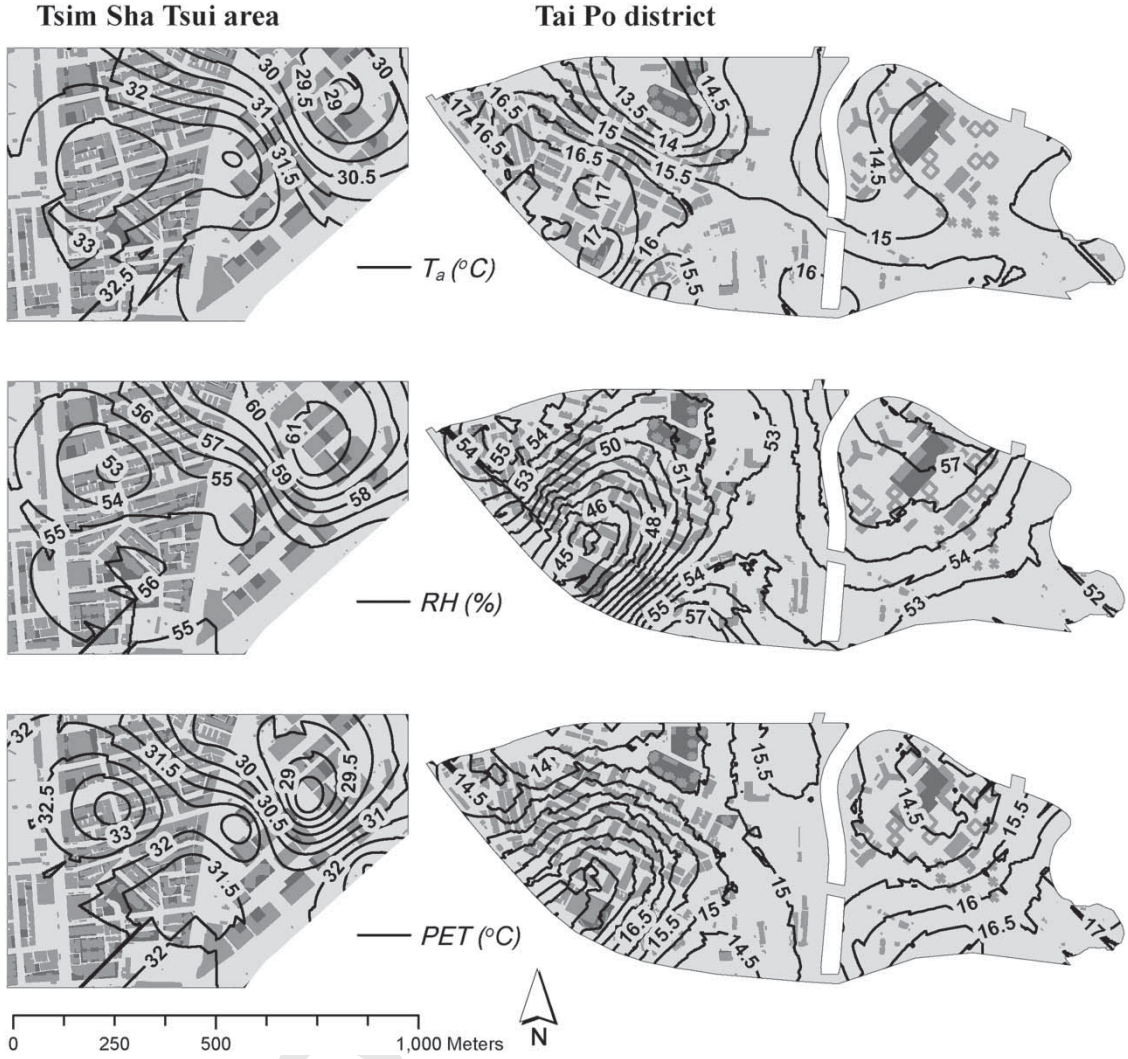

Figure 8. The estimated spatially continuous data of T_a, RH and PET generated based on corresponding optimal interpolation methods of two study areas respectively.

respectively. Down to the building scale, a quantitative building design guideline APP-152 (BD 2011) has been developed for guiding and selecting an appropriate building configuration and lay out for fostering a quality and sustainable built environment in Hong Kong. However, there is still a missing link at microscale.

To fill the missing link, this study demonstrates a pragmatic and more quantitative method for exploring the spatial distribution of microclimate and thermal conditions of high-density urban areas at microscale by employing real measured data. Using the optimal geo-mapping method, this study turns the obscure and abstract climatic data forms into distinct and concise colourful maps (Figure 8). It will not only be able to provide architects and planners with climatic-environmental background information for conducting AVA and APP-152, but also help policy decision makers to identify environmental hotspots at district level where need to be improved by taking proper actions. Since the study output is managed in GIS, such information enables the integration of climatic design strategies into daily architectural and urban planning practices. Future work of the study includes considering more detailed design measures and conducting longer-term microclimatic surveys.

Acknowledgements

The study is supported by an Early Career Schem Project Grant 2013/14 (Project No.: RGC-ECS458413, named "Applying "Local Climate Zone (LCZ)" into High-density High-rise Cities – A Case Study in Hong Kong") of Hong Kong Research Grants Council. The authors wish to thank Prof. Lutz Katzschner for preparing and conducting field measurements and Mr. Max Lee for calibrating and setting the equipment. In particular, the authors wish to thank Dr. Kevin Lau for giving his advice on academic paper writing. The authors also wish to give special thanks to the referees for their valuable comments which help to improve the paper a lot.

Disclosure statement

No potential conflict of interest was reported by the authors.

References

Andrade, H., and M.-J. Alcoforado. 2008. "Microclimatic Variation of Thermal Comfort in a District of Lisbon (Telheiras) at Night." *Theoretical and Applied Climatology* 92 (3–4): 225–237. doi:10.1007/s00704-007-0321-5.

Apaydin, Halit, F. Kemal Sonmez, and Y. Ersoy Yildirim. 2004. "Spatial Interpolation Techniques for Climate Data in the GAP Region in Turkey." *Climate Research* 28 (1): 31–40. doi:10.3354/cr028031.

ASHRAE, ANSI. 2004. "Standard 55–2004, Thermal Environmental Conditions for Human Occupancy." Atlanta: American Society of Heating, Refrigerating, and Air-conditioning Engineers.

BD. 2011. APP-152 Sustainable Building Design Guidelines, Practice Note for Authorized Persons, Registered Structural Engineers and Registered Geotechnical Engineers. Buildings Department.

Boer, Eric P. J., Kirsten M. de Beurs, and A. Dewi Hartkamp. 2001. "Kriging and thin Plate Splines for Mapping Climate Variables." *International Journal of Applied Earth Observation and Geoinformation* 3 (2): 146–154. doi:10.1016/S0303-2434(01)85006-6.

Bruse, Michael. 1999. "Modelling and Strategies for Improved Urban Climates." Paper read at Invited Paper. Proceedings of the International Conference on Urban Climatology & International Congress of Biometeorology, Sydney.

Bruse, M. 2014. *ENVI-met V3. 1BETA, a Microscale Urban Climate Model,[Online], www.envi-met. com*. Michael Bruse & Team 2009 [cited 19 March 2014].

Bruse, Michael, and Heribert Fleer. 1998. "Simulating Surface–Plant–Air Interactions Inside Urban Environments with a Three Dimensional Numerical Model." *Environmental Modelling & Software* 13 (3): 373–384.

Cena, K., and J. A. Clark. 1981. *Bioengineering, Thermal Physiology and Comfort*. Elsevier Science.

Chan, E. Y., W. B. Goggins, J. J. Kim, and S. M. Griffiths. 2012. "A Study of Intracity Variation of Temperature-related Mortality and Socioeconomic Status Among the Chinese Population in Hong Kong." *Journal of Epidemiology & Community Health* 66 (4): 322–327. doi:10.1136/jech.2008.085167.

Chen, Liang, and Edward Ng. 2012. "Simulation of the Effect of Downtown Greenery on Thermal Comfort in Subtropical Climate Using PET Index: A Case Study in Hong Kong." *Architectural Science Review* 56 (4): 297–305. doi:10.1080/00038628.2012.684871.

Chen, Liang, Edward Ng, Xipo An, Chao Ren, Max Lee, Una Wang, and Zhengjun He. 2012. "Sky View Factor Analysis of Street Canyons and its Implications for Daytime Intra-urban Air Temperature Differentials in High-rise, High-density Urban Areas of Hong Kong: A GIS-based Simulation Approach." *International Journal of Climatology* 32 (1): 121–136. doi:10.1002/joc.2243.

Cheng, Vicky, Edward Ng, Cecilia Chan, and Baruch Givoni. 2012. "Outdoor Thermal Comfort Study in a Sub-tropical Climate: A Longitudinal Study Based in Hong Kong." *International Journal of Biometeorology* 56 (1): 43–56. doi:10.1007/s00484-010-0396-z.

Crawford, Jenny, and Simin Davoudi. 2009. *Planning for Climate Change: Strategies for Mitigation and Adaptation for Spatial Planners*. Routledge.

Cressie, Noel. 1986. "Kriging Nonstationary Data." *Journal of the American Statistical Association* 81 (395): 625–634. doi:10.1080/01621459.1986.10478315.

De Schiller, Silvia, and John Martin Evans. 1996. "Training Architects and Planners to Design with Urban Microclimates." *Atmospheric Environment* 30 (3): 449–454.

Erell, Evyatar, David Pearlmutter, T. Terry, and J. Williamson. 2011. *Urban Microclimate: Designing the Spaces between Buildings*. Routledge.

Fan, Hongli, and David J. Sailor. 2005. "Modeling the Impacts of Anthropogenic Heating on the Urban Climate of Philadelphia: A Comparison of Implementations in two PBL Schemes." *Atmospheric Environment* 39 (1): 73–84. doi:10.1016/j.atmosenv.2004.09.031.

Hartkamp, A. Dewi, Kirsten De Beurs, Alfred Stein, and Jeffrey W. White. 1999. *Interpolation Techniques for Climate Variables*. CIMMYT Mexico: DF.

Hengl, Tomislav. 2007. "A Practical Guide to Geostatistical Mapping of Environmental Variables." In *JRC Scientific and Technical Reports. European Commission, Joint Research Centre*. Luxemburg.

Höppe, P. 1999. "The Physiological Equivalent Temperature – A Universal Index for the Biometeorological Assessment of the Thermal Environment." *International Journal of Biometeorology* 43 (2): 71–75. doi:10.1007/s004840050118.

Humphreys, Michael A. 1977. "The Optimum Diameter for a Globe Thermometer for Use Indoors." *Annals of Occupational Hygiene* 20 (2): 135–140.

Huttner, Sebastian, Michael Bruse, and Paul Dostal. 2008. "Using ENVI-Met to Simulate the Impact of Global Warming on the Microclimate in Central European Cities." *Ber Meteorol Inst Univ Freiburg* 18: 307–312.

Ichinose, Toshiaki, Kazuhiro Shimodozono, and Keisuke Hanaki. 1999. "Impact of Anthropogenic Heat on Urban Climate in Tokyo." *Atmospheric Environment* 33 (24–25): 3897–3909. doi:10.1016/S1352-2310(99)00132-6.

ISO. 1998. *ISO 7726: Ergonomics of the Thermal Environment-instruments for Measuring Physical Quantities*. Geneva: International Standard Organization.

Johnston, Kevin, Jay M. Ver Hoef, Konstantin Krivoruchko, and Neil Lucas. 2001. *Using ArcGIS Geostatistical Analyst*. Vol. 380: Esri Redlands.

Kántor, Noémi, and János Unger. 2010. "Benefits and Opportunities of Adopting GIS in Thermal Comfort Studies in Resting Places: An Urban Park as an Example." *Landscape and Urban Planning* 98 (1): 36–46. doi:10.1016/j.landurbplan.2010.07.008.

Kato, Soushi, and Yasushi Yamaguchi. 2005. "Analysis of Urban Heat-Island Effect Using ASTER and ETM + Data: Separation of Anthropogenic Heat Discharge and Natural Heat Radiation from Sensible Heat Flux." *Remote Sensing of Environment* 99 (1–2): 44–54. doi:10.1016/j.rse.2005.04.026.

Li, Jin, and Andrew D. Heap. 2008. *A Review of Spatial Interpolation Methods for Environmental Scientists*. Canberra: Geoscience Australia.

Man Sing, Wong, Yang Jinxin, J. Nichol, Weng Qihao, M. Menenti, and P. W. Chan. 2015. "Modeling of Anthropogenic Heat Flux Using HJ-1B Chinese Small Satellite Image: A Study of Heterogeneous Urbanized Areas in Hong Kong." *IEEE Geoscience and Remote Sensing Letters* 12 (7): 1466–1470. doi:10.1109/LGRS.2015.2409111.

Mayer, H., and P. Höppe. 1987. "Thermal Comfort of Man in Different Urban Environments." *Theoretical and Applied Climatology* 38 (1): 43–49.

Nalder, Ian A., and Ross W. Wein. 1998. "Spatial Interpolation of Climatic Normals: Test of a New Method in the Canadian

Boreal Forest." *Agricultural and Forest Meteorology* 92 (4): 211–225.

Ng, Edward. 2009. "Policies and Technical Guidelines for Urban Planning of High-density Cities–air Ventilation Assessment (AVA) of Hong Kong." *Building and Environment* 44 (7): 1478–1488.

Ng, Edward. 2012. "Towards Planning and Practical Understanding of the Need for Meteorological and Climatic Information in the Design of High-density Cities: A Case-based Study of Hong Kong." *International Journal of Climatology* 32 (4): 582–598.

Ng, Edward, Liang Chen, Yingna Wang, and Chao Yuan. 2012. "A Study on the Cooling Effects of Greening in a High-density City: An Experience from Hong Kong." *Building and Environment* 47: 256–271.

Ng, Edward, and Vicky Cheng. 2012. "Urban Human Thermal Comfort in Hot and Humid Hong Kong." *Energy and Buildings* 55 (0): 51–65. doi:10.1016/j.enbuild.2011.09.025.

Ng, Edward, V. Cheng, and C. Chan. 2008. Urban Climatic Map and Standards for Wind Environment – Feasibility Study. Technical Input Report.

Ng, Edward, and Chao Ren. 2012. *Final Report – Wind Standard, Urban Climatic Map and Standards for Wind Environment – Feasibility Study*. Hong Kong: Report for Planning Department of Hong Kong Government.

Nikolopoulou, M., N. Baker, and K. Steemers. 1999. "Improvements to the globe thermometer for outdoor use." *Architectural Science Review* 42 (1): 27–34.

Oke, Tim R. 1981. "Canyon Geometry and the Nocturnal Urban Heat Island: Comparison of Scale Model and Field Observations." *Journal of Climatology* 1 (3): 237–254.

Oke, TR. 1988. "Street Design and Urban Canopy Layer Climate." *Energy and Buildings* 11 (1): 103–113.

Oke, Timothy R. 1997. "Urban Environments." *The Surface Climates of Canada*, 303–327.

Oke, Tim R. 2004. *Initial Guidance to Obtain Representative Meteorological Observations at Urban Sites*. Vol. 81. World Meteorological Organization Geneva.

Oliveira, Sandra, and Henrique Andrade. 2007. "An Initial Assessment of the Bioclimatic Comfort in an Outdoor Public Space in Lisbon." *International Journal of Biometeorology* 52 (1): 69–84. doi:10.1007/s00484-007-0100-0.

Penwarden, A. D., and A. E. E. Wise. 1975. *Wind Environment Around Buildings*. Building Research Establishment Report. London: Department of the Environment, Building Research Establishment. Her Majesty's Stationery Office.

Ren, Chao, Yingsheng Zheng, Yuan Shi, Kevin Lau, Steve Yim, Justin Ho, and Edward Ng. 2015. Applying "Local Climate Zone (LCZ)" into a High-density High-rise Cities – A Case Study in Hong Kong. In *9th International Conference on Urban Climate jointly with 12th Symposium on the Urban Environment*. Toulouse France: International Association for Urban Climate (IAUC) and the American Meteorological Society (AMS).

Robinson, D. 2012. *Computer Modelling for Sustainable Urban Design: Physical Principles, Methods and Applications*. Taylor & Francis.

Saaroni, Hadas, Eyal Ben-Dor, Arieh Bitan, and Oded Potchter. 2000. "Spatial Distribution and Microscale Characteristics of the Urban Heat Island in Tel-Aviv, Israel." *Landscape and Urban Planning* 48 (1–2): 1–18. doi:10.1016/S0169-2046(99)00075-4.

Santamouris, Matheos, and Francis Allard. 1998. *Natural Ventilation in Buildings: A Design Handbook*. Earthscan.

Santamouris, M., N. Papanikolaou, I. Livada, I. Koronakis, C. Georgakis, A. Argiriou, and D. N. Assimakopoulos. 2001. "On the Impact of Urban Climate on the Energy Consumption of Buildings." *Solar Energy* 70 (3): 201–216. doi:10.1016/S0038-092X(00)00095-5.

Stewart, I. D., and T. R. Oke. 2012. "Local Climate Zones for Urban Temperature Studies." *Bulletin of the American Meteorological Society* 93 (12): 1879–1900. doi:10.1175/bams-d-11-00019.1.

Svensson, Marie K. 2004. "Sky View Factor Analysis – Implications for Urban Air Temperature Differences." *Meteorological Applications* 11 (03): 201–211.

UN. 2014. *World Urbanization Prospects, The 2014 Revision*. New York: UN, Department of Economic and Social Affairs United Nations, Population Division.

Watson, I. D., and G. T. Johnson. 1987. "Graphical Estimation of Sky View-factors in Urban Environments." *Journal of Climatology* 7 (2): 193–197. doi:10.1002/joc.3370070210.

Webster, Richard, and Margaret Oliver. 2001. *Geostatistics for Environmental Scientists (Statistics in Practice)*. Wiley.

WHO. 2003. *Climate Change and Human Health: Risks and Responses*. Geneva: World Health Organization.

Zhang, Kai, Evan M. Oswald, Daniel G. Brown, Shannon J. Brines, Carina J. Gronlund, Jalonne L. White-Newsome, Richard B. Rood, and Marie S. O'Neill. 2011. "Geostatistical Exploration of Spatial Variation of Summertime Temperatures in the Detroit Metropolitan Region." *Environmental Research* 111 (8): 1046–1053. doi:10.1016/j.envres.2011.08.012.